Hindawi
Journal of Chemistry
Volume 2022, Article ID 7087110, 21 pages
https://doi.org/10.1155/2022/7087110

Research Article

Chemical Constituents from *Uapaca guineensis* (Phyllanthaceae), and the Computational Validation of Their Antileishmanial and Anti-inflammatory Potencies

Gervais Mouthé Happi,[1] **Mireille Towa Yimtchui**,[2] **Sikiru Akinyeye Ahmed**,[3] **Shina Salau**,[3] **Liliane Clotilde Dzouemo**,[2] **Klev Gaïtan Sikam**,[2] **and Jean Duplex Wansi**[2]

[1]*Department of Chemistry, Higher Teacher Training College, The University of Bamenda, P.O. Box 39, Bambili, Cameroon*
[2]*Department of Chemistry, Faculty of Sciences, University of Douala, P.O. Box 24157, Douala, Cameroon*
[3]*Department of Chemistry and Industrial Chemistry, Kwara State University, Malete, P.M.B 1530, Ilorin 23431, Nigeria*

Correspondence should be addressed to Gervais Mouthé Happi; gervais20022003@yahoo.fr

Received 27 August 2022; Accepted 11 October 2022; Published 26 October 2022

Academic Editor: Ashutosh Sharma

From the chemical investigations of the root bark of *Uapaca guineensis*, nine distinct compounds (**1**–**9**) have been isolated and characterized as lupeol, betulin, betulinic acid, *β*-amyryl acetate, physcion, quercetin, rutin, *β*-sitosterol, and *β*-sitosterol-3-*O*-*β*-D-glucopyranoside, respectively. The structures of all the isolated compounds have been established using their NMR data as well as the comparison of those data with the ones reported in the literature. Interestingly, to the best of our knowledge, except for the lupane-type triterpenoids (**1**–**3**) and compounds **4** and **9**, all the other compounds are reported for the first time from this genus. Since the plant is widely used for the treatment of skin diseases, leishmaniasis and inflammatory diseases, the anti-leishmanial and anti-inflammatory potencies of all the isolated compounds have been computationally validated through their ability to inhibit the receptors 1QCC and 2XOX (for the antileishmanial studies) and 6Y3C and 1CX2 (for the anti-inflammatory studies). Furthermore, the ADMET studies of compounds have been done to evaluate their drug-likeness. Results demonstrate that all the isolated compounds showed a better affinity for both receptors' binding sites than the standard drugs miltefosine and aspirin. Moreover, the compounds would not cause addiction when used as lead molecules whereas, aspirin is predicted to violate the BBB over a long term of usage as a drug. This study gives additional information on the chemistry of *U. guineensis* and its classification as a potential source of good leads for the development of potent antileishmanial and anti-inflammatory drugs.

1. Introduction

Leishmaniasis has been classified in 2018 as one of the most neglected tropical diseases infecting one billion people in 149 countries around the world due to its high incidence, morbidity, and mortality [1]. It is a vector-borne disease caused by one of the 29 species of the protozoan *Leishmania* spp. including *Leishmania donovani* and *Leishmania infantum,* which are transmitted by the bites of the female phlebotomine sandfly and are responsible for the more severe forms of the diseases leading to the high rates of death [2]. The current existing and prescribed drugs are toxic, expensive in cost, not sufficiently efficient, long duration of treatment, and face parasite resistance in many cases [3]. Furthermore, the literature reveals that the mechanism of the development of the pathogenicity of the parasite *Leishmania* spp. in its host is done through the inhibition of proinflammatory responses and the suppression of nitric oxide (NO) production [4]. However, inflammation-related chronic diseases like arthritis and irritable bowel syndrome represent an important concern for public health affecting a larger and ever-growing population [5]. The nonsteroidal anti-inflammatory drugs, which are mostly prescribed as therapeutics, display several side effects, including

gastrointestinal, cardiovascular, or renal complications [6]. All this evidence highlights the actual need for developing prototype drugs that are more effective and less toxic to complement or replace the existing ones. For several decades, medicinal plants have been demonstrated to be a good reservoir of potent leads in the development of new effective drugs [7, 8].

Uapaca guineensis is a tree whose wood is traded under the name "Rikio." The tree is up to 30 m high, 80 cm in diameter, and has a bole straight, irregular, and up to 15 m long with large ascending branches carrying leaves which are simple, alternate, erect, and grouped at the ends of the branches. The male flowers consist of 6–9 whitish or greenish bracts surrounding stamens while the female ones do not have petals, but their globose ovary is surmounted by 3 styles. The fruits are globose drupes up to 3 cm in diameter, weighing about 7 g, greenish-yellow when ripe, then brown [9]. The plant is used in traditional popular medicine for the treatment of several infections including skin diseases like leprosy, eczema, and leishmaniasis; for the management of inflammatory diseases like rheumatism and joint pains, as well as purgative, gastrointestinal troubles, antiabortive, aphrodisiac, or the treatment of malaria [10]. Therefore, based on its traditional uses, the plant might be a good source of specialized metabolites with antileishmanial and anti-inflammatory potencies. As part of our program of investigations of Cameroonian medicinal plants for their bioactive compounds, we have chemically investigated the root bark of *U. guineensis* and computationally validated the antileishmanial and anti-inflammatory potencies of the isolated compounds. In addition, their ADMET (absorption, distribution, metabolism, excretion, and toxicity) studies have been performed in order to provide more insights into how those compounds are processed by a living organism.

2. Experimental

2.1. General Instrumentation. EI-MS was recorded on a Finnigan LCQ with a Rheos 4000 quaternary pump (Flux Instrument). The ^{1}H and ^{13}C-NMR spectra were recorded on a Bruker Advance III 500 MHz NMR spectrometer (Bruker, Rheinstetten, Germany) equipped with a 5 mm cryogenic DCH (^{1}H/^{13}C) probe. Chemical shifts are reported in parts per million (δ) using tetramethylsilane (TMS) (Sigma-Aldrich, Munich, Germany) as the internal standard, while coupling constants (J) were measured in Hz. Column chromatography was carried out on silica gel 230–400 mesh, Merck, (Merck, Darmstadt, Germany) and silica gel 70–230 mesh (Merck). Thin layer chromatography (TLC) was performed on Merck precoated silica gel 60 F_{254} aluminium foil (Merck), and spots were detected using diluted sulphuric acid spray reagent before heating. All reagents used were of analytical grade.

2.2. Plant Material. The root bark of *Uapaca guineensis* Müll. Arg. (Phyllanthaceae) was harvested in June 2021 along the borders of the river Nyong at Mengueme (GPS coordinates: Latitude 3°15′28″N, Longitude 11°08′28″E, Elevation: 343 m), Centre Region of Cameroon. The plant was identified by a specialist of the National Herbarium of Cameroon in Yaounde and compared with a voucher formerly kept under the registration number No. 41501/HNC.

2.3. Extraction and Isolation. The air-dried and powdered root bark (1800 g) of *U. guineensis* was extracted twice with methanol (7 L) for 72 h and 48 h, respectively. After decantation, filtration, and evaporation of the solvent under reduced pressure, 88.4 g of crude extract were obtained, dissolved in water and successively partitioned with ethyl acetate and n-butanol to obtain two fractions labelled A (40.3 g) and B (19.4 g), respectively.

The main fraction A was subjected to a silica gel column chromatography eluting with a stepwise gradient of hexane-ethyl acetate (1 : 0 ⟶ 0 : 1, v/v), followed by ethyl acetate - methanol (1 : 0 ⟶ 8 : 2, v/v) to afford six subfractions labelled S_1–S_6, along with eight compounds including β-sitosterol (**8**) (12 mg, hexane/ethyl acetate 19 : 1), β-amyryl acetate (**4**) (8 mg, hexane/ethyl acetate 37 : 3), lupeol (**1**) (14 mg, hexane/ethyl acetate 9 : 1), physcion (**5**) (4 mg, hexane/ethyl acetate 17 : 3), betulin (**2**) (20 mg, hexane/ethyl acetate 8 : 2), betulinic acid (**3**) (7 mg, hexane/ethyl acetate 13 : 7), quercetin (**6**) (5 mg, hexane/ethyl acetate 2 : 3), and β-sitosterol-3-*O*-β-D-glucopyranoside (**9**) (10 mg, hexane/ethyl acetate 1 : 4).

Furthermore, the two subfractions S_5 and S_6 showed similar TLC profiles to the fraction B. The three extracts were combined and further purified by silica gel column chromatography eluting with a stepwise gradient of ethyl acetate–methanol (1 : 0 ⟶ 7 : 3, v/v) to afford β-sitosterol-3-*O*-β-D-glucopyranoside (**9**) (10 mg, ethyl acetate) and rutin (**7**) (4 mg, ethyl acetate/methanol 19 : 1).

2.4. Physico-chemical Properties of Isolated Compounds. The physical aspects and the 1D-NMR (^{1}H and ^{13}C) data of all the isolated compounds are presented as follows:

Lupeol (**1**)–White powder. ^{1}H NMR ($CDCl_3$, 500 MHz) δ: 4.71 (1H, *d*, J = 4.0 Hz, H-29b), 4.69 (1H, *d*, J = 4.0 Hz, H-29a), 3.21 (1H, dd, J = 11.5, 4.7 Hz, H-3), 2.41 (1H, *m*, H-19), 1.93 (1H, *m*, H-21b), 1.70 (3H, *s*, H-30), 1.69 (1H, *m*, H-15b), 1.67 (3H, *m*, H-1b, H-12b, H-13), 1.62 (1H, *m*, H-2a), 1.59 (1H, *m*, H-2b), 1.52 (1H, *m*, H-6a), 1.47 (1H, *m*, H-16b), 1.43 (1H, *m*, H-11a), 1.42 (1H, *m*, H-6b), 1.41 (2H, *m*, H-7), 1.40 (1H, *m*, H-22b), 1.39 (1H, *m*, H-18), 1.38 (1H, *m*, H-16a), 1.33 (1H, *m*, H-21a), 1.28 (1H, *m*, H-9), 1.23 (1H, *m*, H-11b), 1.21 (1H, *m*, H-22a), 1.07 (3H, *s*, H-26), 1.05 (1H, *m*, H-12a), 0.99 (1H, *m*, H-15a), 0.97 (3H, *s*, H-27), 0.95 (3H, *s*, H-28), 0.92 (1H, *m*, H-1a), 0.86 (3H, *s*, H-25), 0.81 (3H, *s*, H-24), 0.78 (3H, *s*, H-23), 0.72 (1H, *m*, H-5); ^{13}C NMR ($CDCl_3$, 125 MHz) δ: 148.2 (C-20), 109.5 (C-29), 79.0 (C-3), 55.1 (C-5), 53.9 (C-18), 50.1 (C-9), 48.7 (C-17), 47.9 (C-19), 44.2 (C-22), 42.3 (C-14), 41.7 (C-8), 40.2 (C-16), 38.9 (C-1), 38.7 (C-4), 37.1 (C-10), 33.4 (C-7), 32.7 (C-13), 28.0 (C-23), 27.4 (C-2, C-21, C-15), 23.9

Table 1: Vina search space specified for receptor-ligand docking in this study.

S/N	Receptors code	Dimension (Å)	Center (Å)
1	1QCC.pdb	*X*: 20.14, *Y*: 20.14, *Z*: 20.14	*X*: 22.84, *Y*: 23.66, *Z*: 12.557
2	2XOX.pdb	*X*: 22.34, *Y*: 22.35, *Z*: 22.35	*X*: 36.64, *Y*: 43.22, *Z*: 19.11
3	6Y3C.pdb	*X*: 40.21, *Y*: 40.21, *Z*: 40.21	*X*: −47.97, *Y*: -53.19, *Z*: −2.632
4	1CX2.pdb	*X*: 39.35, *Y*: 39.35, *Z*: 39.35	*X*: 28.02, *Y*: 13.50, *Z*: 39.54

(C-12), 20.9 (C-11), 19.6 (C-30), 18.4 (C-6), 16.9 (C-28), 16.6 (C-25), 15.9 (C-26), 15.4 (C-24), 15.1 (C-27).

Betulin (**2**)–White amorphous powder. ^{1}H NMR ($CDCl_3$, 500 MHz) δ: 4.67 (1H, *d*, J = 4.0 Hz, H-29b), 4.51 (1H, *d*, J = 4.0 Hz, H-29a), 3.79 (1H, *d*, J = 10.8 Hz, H-28b), 3.31 (1H, *d*, J = 10.8 Hz, H-28a), 3.16 (1H, dd, J = 10.5, 5.0 Hz, H-3), 1.69 (3H, *s*, H-30), 1.64 (1H, *m*, H-2a), 1.62 (1H, *m*, H-1b), 1.60 (1H, *m*, H-2b), 1.01 (3H, *s*, H-27), 0.99 (3H, *s*, H-26), 0.96 (3H, *s*, H-23), 0.91 (1H, *m*, H-1a), 0.82 (3H, *s*, H-25), 0.76 (3H, *s*, H-24), 0.66 (1H, *m*, H-5); ^{13}C NMR ($CDCl_3$, 125 MHz) δ: 150.5 (C-20), 109.8 (C-29), 79.0 (C-3), 60.5 (C-28), 53.3 (C-5), 50.5 (C-9), 48.8 (C-19), 47.9 (C-18), 47.7 (C-17), 42.6 (C-14), 41.1 (C-8), 39.7 (C-1), 38.8 (C-4), 37.3 (C-13), 37.1 (C-10), 34.4 (C-7), 34.0 (C-22), 29.7 (C-21), 29.3 (C-16), 28.0 (C-23), 27.6 (C-2), 27.4 (C-15), 25.3 (C-12), 20.9 (C-11), 19.6 (C-30), 18.4 (C-6), 16.1 (C-27), 16.1 (C-25), 16.1 (C-24), 16.0 (C-26).

Betulinic acid (**3**)–White powder. ^{1}H NMR ($CD_3OD + CDCl_3$, 500 MHz) δ: 4.71 (1H, *m*, H-29a), 4.58 (1H, *m*, H-29b), 3.31 (1H, ddd, J = 5.0, 16.9, 10.5 Hz, H-19), 3.21 (1H, dd, J = 11.5, 4.7 Hz, H-3), 2.35 (1H, *m*, H-13), 2.24 (1H, *m*, H-16b), 1.94 (1H, *m*, H-15b), 1.69 (3H, *s*, H-30), 1.67 (1H, *m*, H-1b), 1.64 (1H, *m*, H-12b), 1.61 (1H, *m*, H-18), 1.58 (2H, *m*, H-2), 1.52 (1H, *m*, H-6a), 1.42 (1H, *m*, H-6b), 1.41 (1H, *m*, H-11a), 1.40 (1H, *m*, H-16a), 1.39 (2H, *m*, H-7), 1.35 (1H, *m*, H-15a), 1.29 (1H, *m*, H-9), 1.25 (1H, *m*, H-11b), 1.07 (3H, *s*, H-26), 1.03 (1H, *m*, H-12a), 1.01 (3H, *s*, H-27), 0.97 (3H, *s*, H-26), 0.97 (3H, *s*, H-23), 0.92 (1H, *m*, H-1a), 0.86 (3H, *s*, H-25), 0.85 (3H, *s*, H-25), 0.81 (3H, *s*, H-24), 0.78 (3H, *s*, H-23), 0.76 (3H, *s*, H-24), 0.72 (1H, *m*, H-5); ^{13}C NMR ($CD_3OD + CDCl_3$, 125 MHz) δ: 179.7 (C-28), 152.2 (C-20), 110.8 (C-29), 78.9 (C-3), 57.5 (C-17), 56.1 (C-5), 50.5 (C-9), 49.2 (C-19), 46.9 (C-18), 42.3 (C-14), 40.7 (C-8), 38.8 (C-4), 38.7 (C-13), 38.7 (C-1), 37.1 (C-10), 37.0 (C-22), 34.4 (C-7), 32.3 (C-16), 30.4 (C-15), 29.7 (C-21), 28.0 (C-23), 27.9 (C-2), 25.3 (C-12), 20.9 (C-11), 19.6 (C-30), 18.4 (C-6), 15.9 (C-26), 15.8 (C-25), 15.4 (C-24), 15.0 (C-27).

β-amyryl acetate (**4**)–White powder. ^{1}H NMR ($CDCl_3$, 500 MHz) δ: 5.03 (1H, *t*, J = 4.0 Hz, H-12), 4.32 (1H, *m*, H-3), 2.13 (3H, *s*, H-2′), 1.75 (1H, *dd*, J = 13.6 Hz, 4.6 Hz, H-18), 0.93 (3H, *s*, H-27), 0.82 (3H, *s*, H-28), 0.72 (3H, *s*, H-25), 0.71 (3H, *s*, H-26), 0.65 (3H, *s*, H-30), 0.64 (3H, *s*, H-29), 0.64 (3H, *s*, H-24), 0.63 (3H, *s*, H-23). ^{13}C NMR ($CDCl_3$, 125 MHz) δ: 171.9 (C-1′), 144.3 (C-13), 122.4 (C-12), 79.8 (C-3), 55.4 (C-5), 47.5 (C-9), 42.5 (C-18), 41.7 (C-14), 39.8 (C-8), 37.5 (C-4), 35.8 (C-22), 34.5 (C-10), 33.2 (C-29), 30.9 (C-17), 28.3 (C-24), 28.1 (C-1), 26.1 (C-28), 25.9 (C-27), 25.5 (C-15), 23.6 (C-2), 23.0 (C-23), 21.9 (C-16), 20.8 (C-2′), 16.8 (C-26), 16.6 (C-30), 15.6 (C-25).

Physcion (**5**)–Yellowish powder. ^{1}H NMR ($CDCl_3$, 500 MHz) δ: 12.25 (1H, *s*, OH-8), 12.05 (1H, *s*, OH-1), 7.56 (1H, *d*, J = 2.0 Hz, H-4), 7.30 (1H, *d*, J = 2.1 Hz, H-5), 7.02 (1H, *d*, J = 2.0 Hz, H-2), 6.62 (1H, *d*, J = 2.1 Hz, H-7), 3.87 (3H, *s*, OMe-7), 2.38 (3H, *s*, Me-3). ^{13}C NMR ($CDCl_3$, 125 MHz) δ: 190.8 (C-9), 182.0 (C-10), 166.5 (C-6), 165.1 (C-8), 162.5 (C-1), 148.4 (C-3), 135.2 (C-11), 133.2 (C-14), 124.5 (C-2), 121.3 (C-4), 113.6 (C-13), 110.2 (C-12), 108.2 (C-5), 106.7 (C-7), 56.0 (OMe-6), 22.1 (Me-3).

Quercetin (**6**)–Yellowish powder. ^{1}H NMR (CD_3OD, 500 MHz) δ: 7.74 (1H, *d*, J = 1.9 Hz, H-2′), 7.64 (1H, dd, J = 8.6 Hz, H-6′), 6.91 (1H, *d*, J = 8.6 Hz, H-5′), 6.39 (1H, *d*, J = 1.8 Hz, H-8), 6.23 (1H, *d*, J = 1.8 Hz, H-6). ^{13}C NMR (CD_3OD, 125 MHz) δ: 175.6 (C-4), 164.9 (C-7), 160.7 (C-5), 156.9 (C-8a), 147.4 (C-4′), 146.7 (C-2), 144.6 (C-3′), 135.7 (C-3), 122.9 (C-1′), 120.7 (C-6′), 115.3 (C-5′), 114.7 (C-2′), 103.2 (C-4a), 98.4 (C-6), 93.8 (C-8).

Rutin (**7**)–Yellowish powder. ^{1}H NMR (CD_3OD, 500 MHz) δ: 7.68 (1H, *d*, J = 1.8 Hz, H-2′), 7.65 (1H, dd, J = 7.9 Hz, 1.8 Hz, H-6′), 6.89 (1H, *d*, J = 7.9 Hz, H-5′), 6.42 (1H, *d*, J = 2.0 Hz, H-8), 6.23 (1H, *d*, J = 2.0 Hz, H-6), 5.13 (1H, *d*, J = 8.2 Hz, H-1″/Glu), 4.53 (1H, *d*, J = 7.9 Hz, H-1‴/Rha), 3.82 (1H, *m*, H-6b″/Glu), 3.64 (1H, *m*, H-2‴/Rha), 3.47 (1H, *m*, H-2″/Glu), 3.46 (1H, *m*, H-5‴/Rha), 3.42 (1H, *m*, H-6a″/Glu), 3.29 (1H, *m*, H-4‴/Rha), 1.18 (3H, *d*, J = 6.8 Hz, H-6‴/Rha). ^{13}C NMR (CD_3OD, 125 MHz) δ: 178.0 (C-4), 164.7 (C-7), 161.5 (C-5), 157.9 (C-2), 157.1 (C-8a), 148.4 (C-4′), 144.4 (C-3′), 134.2 (C-3), 122.1 (C-6′), 121.6 (C-1′), 116.2 (C-2′), 114.6 (C-5′), 104.1 (C-4a), 98.5 (C-6), 93.4 (C-8); 6-*O*-Glucosyl: 103.2 (C-1″), 76.7 (C-3″), 74.3 (C-2″), 70.8 (C-5″), 69.9 (C-4″), 67.1 (C-6″); 1-*O*-Rhamnosyl: 101.0 (C-1‴), 75.8 (C-3‴), 72.5 (C-4‴), 70.6 (C-2‴), 68.3 (C-5‴), 16.4 (C-6‴).

β-sitosterol (**8**)–White powder. ^{1}H NMR ($CDCl_3$, 500 MHz) δ: 5.34 (1H, *t*, J = 6.4, H-6), 3.51 (1H, dd, J = 4.5, 4.2 Hz, H-3), 1.23 (3H, *s*, H-19), 1.15 (3H,s, H-18), 1.02 (3H, *d*, J = 6.5 Hz, H-26), 0.92 (3H, *d*, J = 6.3 Hz, H-27), 0.92 (3H,m, H-29), 0.86 (3H, *d*, J = 6.3 Hz, H-21). ^{13}C NMR ($CDCl_3$, 125 MHz) δ: 141.1 (C-5), 121.6 (C-6), 72.2 (C-3), 57.9 (C-14), 56.6 (C-17), 50.4 (C-9), 46.4 (C-24), 42.7 (C-13), 42.6 (C-4), 38.9 (C-12), 37.7 (C-1), 36.8 (C-10), 36.5 (C-20), 34.5 (C-22),

Table 2: Docked scores of isolated compounds.

Compounds	Antileishmanial		Anti-inflammatory	
	1QCC (kcal/mol)	2XOX (kcal/mol)	6Y3C (kcal/mol)	1CX2 (kcal/mol)
1	−7.0	−6.6	−8.0	−7.9
2	−6.3	−6.0	−7.7	−7.4
3	−6.6	−5.9	−7.5	−7.3
4	−7.3	−5.8	−8.5	−8.3
5	−6.6	−7.8	−8.5	−8.2
6	−7.4	−7.7	−8.7	−8.8
7	−7.7	−8.3	−8.9	−9.4
8	−5.7	−6.4	−6.7	−7.5
9	−7.3	−5.2	−8.6	−8.5
Miltefosine	−4.3	−5.0	−6.5	−7.1
Aspirin	−5.3	−5.7	−6.6	−6.9

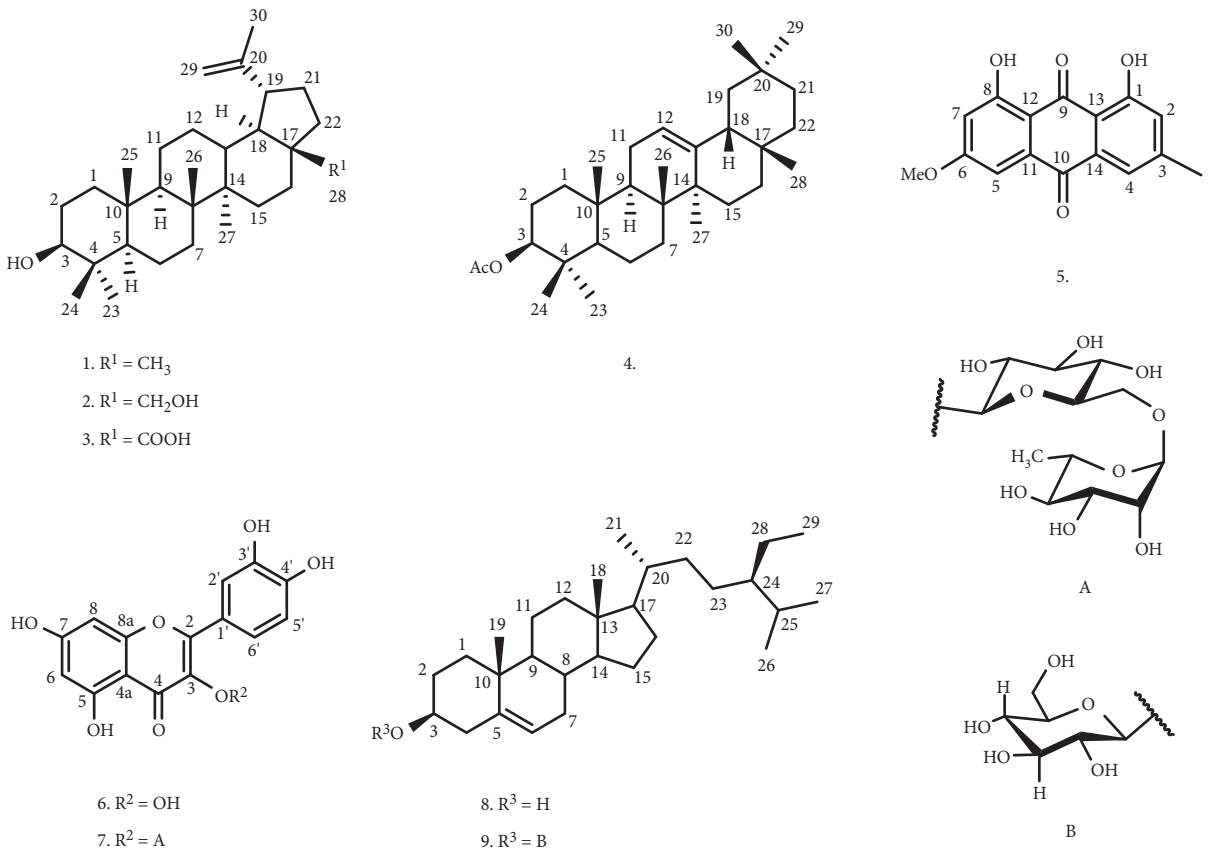

Figure 1: Chemical structures of compounds (**1**–**9**) isolated from *Uapaca guineensis*.

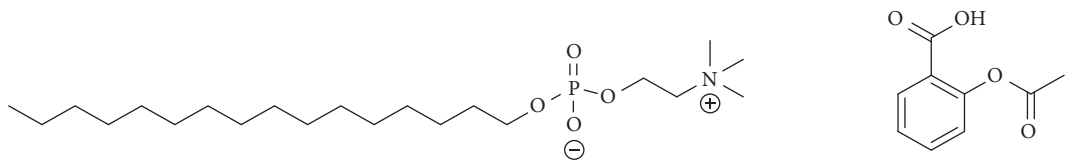

Figure 2: Structures of the standard drugs used during this work.

32.3 (C-7), 32.3 (C-8), 32.1 (C-2), 29.7 (C-25), 28.7 (C-16), 26.5 (C-23), 24.4 (C-15), 23.7 (C-28), 21.4 (C-11), 20.3 (C-26), 19.7 (C-27), 19.5 (C-19), 19.2 (C-21), 12.5 (C-29), 12.4 (C-18).

β-sitosterol-3-*O*-*β*-D-glucopyranoside (**9**)–White powder. ^{1}H NMR ($CD_3OD + CDCl_3$, 500 MHz) δ: 5.32 (2H, *m*, H-6), 4.22 (1H, *d*, $J = 6.5$ Hz, H-1′), 3.67 (1H, *m*, H-6′b), 3.47 (1H, *m*, H-3), 3.44 (1H, *m*, H-6′a), 3.12 (1H, *d*, $J = 7.5$ Hz, H-3′), 3.10 (1H, *m*, H-5′), 3.06 (1H, *m*, H-4′), 2.90 (1H, *t*, $J = 7.0$ Hz, H-2′), 2.12 (1H, *m*, H-20), 1.93 (2H, *m*, H-4), 1.80 (4H, *m*, H-15, H-16), 1.80 (2H, *m*, H-7), 1.63 (1H, *m*, H-27), 1.50 (6H, *m*, H-8, H-9, H-11, H-12), 1.50 (4H, *m*, H-24, H-26), 1.39 (2H, *m*, H-2), 1.24 (2H, *m*, H-1), 1.24 (1H, *m*, H-17), 1.15 (2H, *m*, H-25), 1.15 (1H, *m*, H-14), 0.99 (3H, *d*, $J = 6.9$ Hz, H-29), 0.95 (3H, *s*, H-19), 0.90 (3H, *d*, $J = 6.4$ Hz, H-21), 0.82 (3H, *s*, H-18), 0.76 (3H, *m*, H-28). ^{13}C-NMR ($CD_3OD + CDCl_3$, 125 MHz) δ: 141.0 (C-5), 121.9 (C-6), 102.6 (C-1′), 78.6 (C-3), 78.4 (C-3′), 78.2 (C-5′), 75.4 (C-2′), 71.8 (C-4′), 63.0 (C-6′), 57.0 (C-14), 56.2 (C-17), 51.5 (C-24), 50.4 (C-9), 42.4 (C-4, C-13), 40.8 (C-20), 39.4 (C-12), 37.5 (C-1), 37.0 (C-10), 34.8 (C-22), 32.2 (C-2, C-7), 32.1 (C-8, C-25), 29.3 (C-16), 26.8 (C-23), 25.7 (C-28), 24.6 (C-15), 21.3 (C-21), 19.5 (C-11, C-26), 19.3 (C-27), 19.2 (C-19), 12.5 (C-29), 12.2 (C-18).

2.5. Computational Methodology

2.5.1. Ligands Preparations. A total of nine (9) compounds isolated from *Uapaca guineensis* extract were modelled using Chemdraw® ultra software [11] and optimized at the Molecular Mechanics Force Field '99 (MMFF99) level via the Avogadro® software [12]. Ligands (in an explicit hydrogen state) were then saved in PDBQT format. The standards (i.e., registered drugs), were chosen for comparative analysis with the isolated compounds. Miltefosine® was chosen for the antileishmanial study while Aspirin® was chosen for the anti-inflammation study.

2.5.2. Receptor Preparations. Two receptors namely adenine phosphoribosyltransferase (APRT) (PDB ID: 1QCC) [13] and pteridine reductase (PTR1) (PDB ID: 2XOX) from *Leishmania donovani* [14] were selected for the antileishmanial studies while the receptors human cyclooxygenases 1 and 2 (COX-1 and COX-2) having PDB codes 6Y3C and 1CX2, respectively, were used for the anti-inflammation studies [15, 16]. All four receptors were downloaded from the RCSB database at https://www.rcsb.org. The receptors were pretreated by removing crystallized water molecules and adding polar hydrogens and polar charges using the BIOVIA DS® software 2021 version [17]. The final files were then saved in PDBQT docking-ready format.

2.5.3. Docking Protocol. The binding sites of all four receptors were obtained from their respective associating

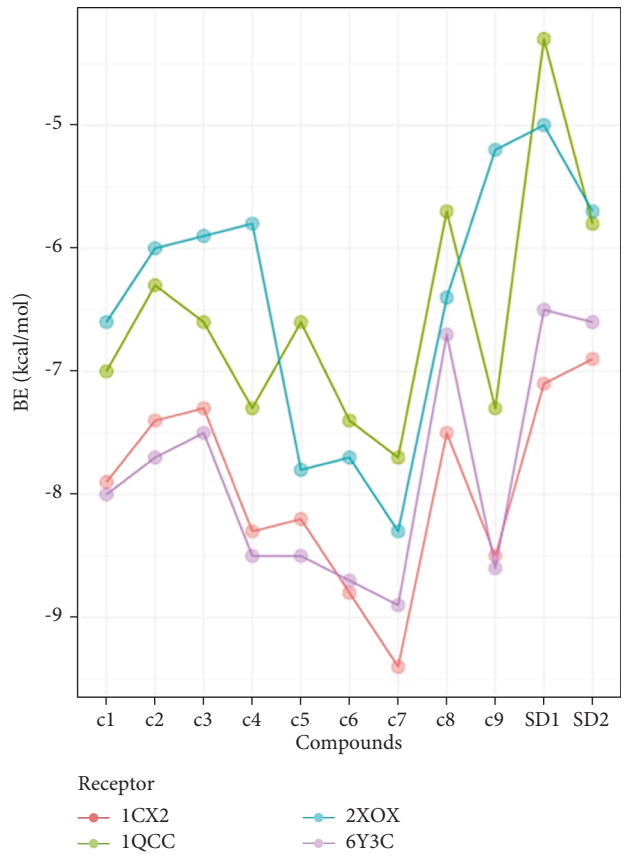

Figure 3: Graphical relationship between isolated compounds and binding energy or binding affinity (BE).

literature which has been deposited at the Protein Data Bank web servers by the crystallographers.

2.5.4. Molecular Docking. Molecular docking was done using the vina/PyRx® software applications [18, 19]. The prepared ligands and prepared receptors were introduced receptor-by-receptor into the PyRx GUI using the vina importing tool.

The mode of docking simulation was specific docking with a flexible method. A search space for the specific docking process was specified for vina. The search space dimensions specified for each receptor are shown in Table 1. The binding affinities of isolated compounds of the *Uapaca guineensis* to the receptors are recorded in Table 2.

2.5.5. Graphical Illustrations. The ligand interaction graphics from the Vina score were snipped from the BIOVIA® DS version 2021 software package [17]. All graphical plots were obtained using the ggplot2® package library [20] in the *R* statistical programming language.

2.5.6. ADMET Property-Prediction. The absorption, distribution, metabolism, excretion, and toxicity property predictions were obtainable from the SMILES index formula of each isolated compounds in the ADMETLab 2.0 [21] web

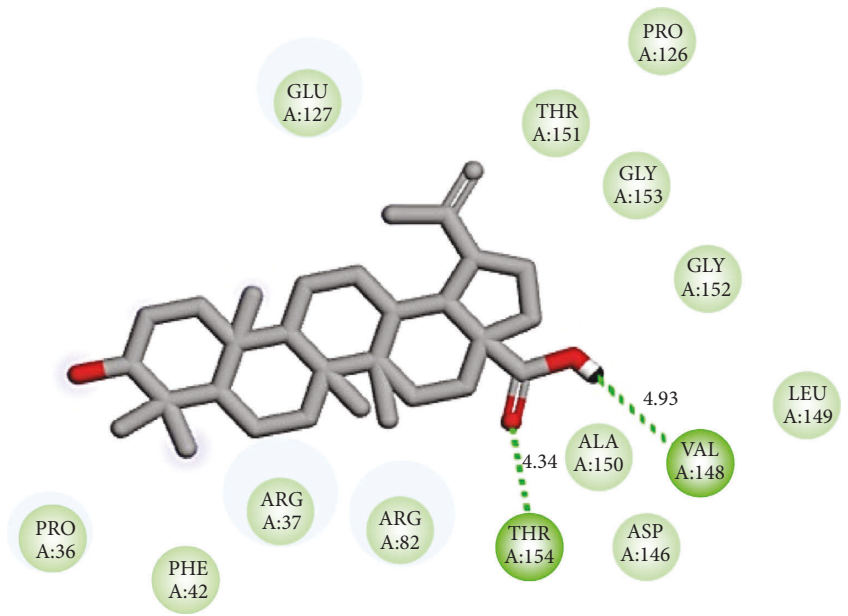

(a)

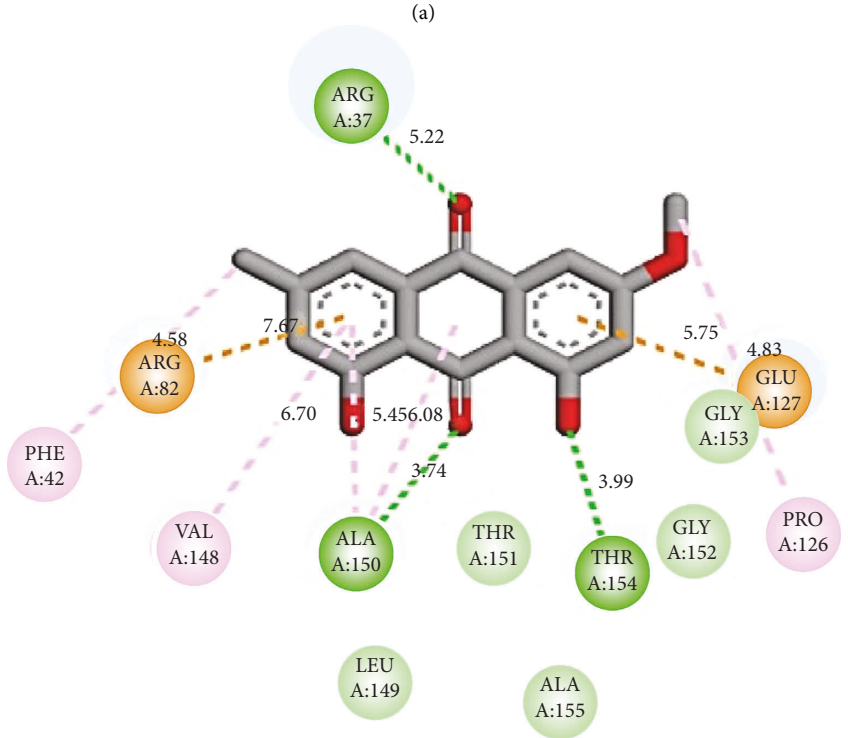

(b)

Figure 4: Continued.

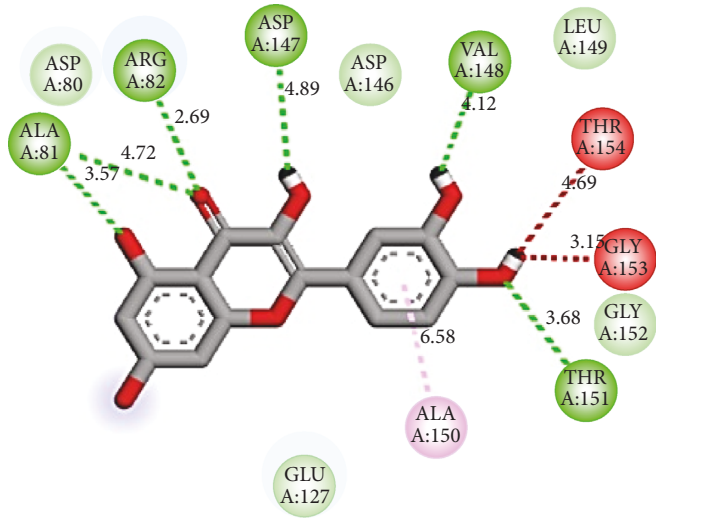

(c)

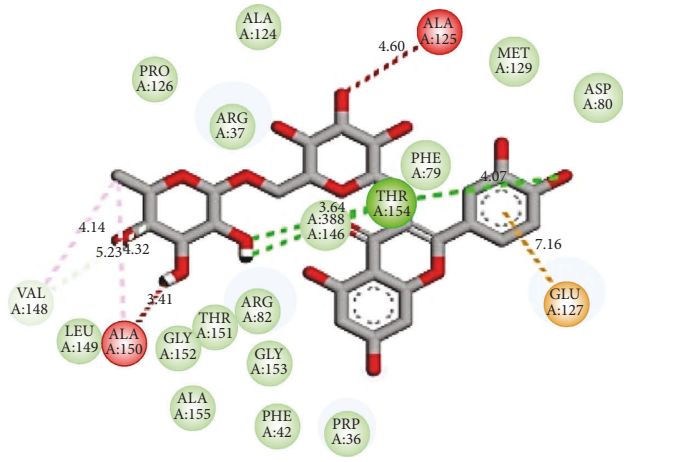

(d)

Figure 4: Continued.

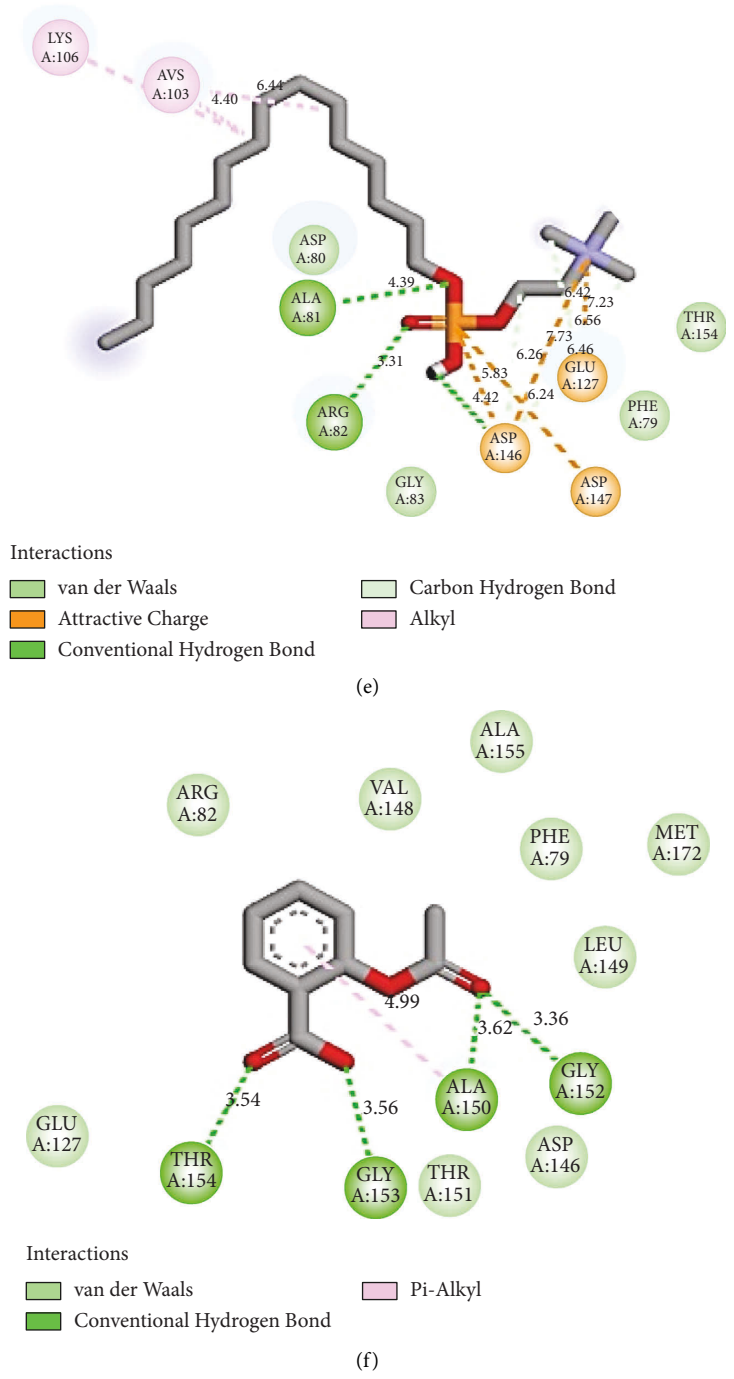

FIGURE 4: Docking poses of selected compounds at the 1QCC receptor binding site–(a) compound **3**, (b) compound **5**, (c) compound **6**, (d) compound **7**, (e) miltefosine, and (f) aspirin.

server. Table 1S (supplementary information file) shows the isolated compound and their smile notations used for the ADMET prediction in this study.

3. Results and Discussion

3.1. Phytochemical Study. The phytochemical investigation of the root bark of *Uapaca guineensis* led to the isolation and identification of nine compounds (Figure 1). Their structures have been established using their spectrometric and spectroscopic data in comparison with those reported in the literature. Thus, the nine compounds have been classified into four triterpenoids including lupeol (**1**) [22, 23], betulin (**2**) [24], betulinic acid (**3**) [25, 26], β-amyryl acetate (**4**) [27]; one anthraquinone named physcion (**5**) [28], two flavonoids identified as quercetin (**6**) and rutin (**7**) [29], as well as two common steroids β-sitosterol (**8**) and its glucoside β-sitosterol-3-*O*-β-D-glucopyranoside (**9**) [30].

Table 3: Conventional hydrogen-bonds of the docked ligand-receptor-interaction.

Compounds	Conventional hydrogen-bonds (length in Å)			
	1QCC	2XOX	6Y3C	1CX2
3	VAL:148 (4.93), THR:154 (4.34)	SER:146 (4.19), ASN:147 (4.24)	GLU:454 (5.38), GLN:203 (6.17)	ASN:382 (4.93), THR:212 (3.86)
5	ARG:37 (5.22), ALA:150 (3.74), THR:154 (3.99)	GLY:13 (3.44), ARG:39 (4.77)	GLN:203 (4.35), ASN:283 (4.88)	THR:208 (5.13)
6	ALA:81 (3.57), ARG:82 (2.69), ASP: 147 (4.89), VAL:148 (4.12), THR:151 (3.68)	ARG:39 (4.96), HIS:36 (3.64), LEU:66 (4.26)	ASN:382 (4.13)	—
7	THR:154 (3.51)	SER:40 (3.96), LYS:16 (3.83), ASN:147 (3.33)	THR:313 (4.23), ASN:382 (4.25)	HIS:214 (5.13), HIS:207 (4.66)
Miltefosine	ALA:81 (4.39), ARG:82 (3.31)	SER:146 (4.16)	VAL:349 (5.23)	HIS:207 (5.25)
Aspirin	THR:154 (3.54), GLY:153 (3.56), ALA:150 (3.62), GLY:152 (3.36)	SER:146 (4.40), SER:146 (3.74)	THR:206 (4.58)	TRP:387 (5.49), ALA:202 (4.33)

Table 4: Predicted ADMET property parameters for the isolated compounds and the selected standards.

Absorption and distribution	1	2	3	4	5	6	7	8	9	SD1	SD2
BBB (±)	−	−	−	−	−	−	−	−	−	−	+
GIA (±)	+	+	+	+	+	+	+	+	-	+	−
Log S	−6.13	−5.74	−6.32	−6.79	−4.55	−3.12	−4.21	−6.88	−4.62	0.051	−1.65
CYP450 2C19 inhibitor	NO	NO	NO	NO	NO	NO	NO	NO	NO	YES	NO
CYP450 1A2 inhibitor	NO	NO	NO	NO	YES	YES	NO	NO	NO	NO	NO
CYP450 3A4 inhibitor	YES	NO	NO	NO	YES	NO	NO	YES	NO	YES	NO
CYP450 2C9 inhibitor	NO	NO	NO	YES	NO	YES	NO	NO	NO	NO	NO
CYP450 2D6 inhibitor	NO	NO	NO	NO	YES	NO	NO	NO	NO	NO	NO
Toxicity											
AMES mutagenesis	NO	NO	NO	NO	NO	NO	NO	NO	NO	NO	NO
Acute oral toxicity rating	III	III	III	III	III	III	III	III	III	II	II
hERG toxicity	NO	NO	NO	NO	NO	NO	NO	YES	YES	YES	NO
Carcinogenicity	NO	NO	NO	NO	NO	NO	NO	NO	NO	NO	NO
Lipinski violation?	NO	NO	NO	NO	NO	YES	NO	YES	NO	YES	YES

SD1, miltefosine, SD2, aspirin.

To the best of our knowledge, all the isolated compounds are reported herein for the first time from this plant species. It is well reported that the genus *Uapaca* is a good source of betulinic acid (**3**) which might be considered as a chemomarker of the genus [31]. Together with its congeners lupeol (**1**) and betulin (**2**), it has been previously isolated from the species *U. paludosa* [32]. Additionally, β-amyryl acetate (**4**), β-sitosterol-3-*O*-β-D-glucopyranoside (**9**), and lupeol (**1**) have been obtained from *U. togoensis* and evaluated for their cytotoxicity towards multifactorial drug-resistant cancer cell lines [33]. Some glucosylated flavonoids namely naringenin-7-*O*-glucoside and kaempferol-3-*O*-glucoside are structurally close to quercetin (**6**) and rutin (**7**) and have been recently isolated for the first time from the ethyl acetate extract of *U. heudelotti* [34]. This study supports the taxonomy of the plant through its chemical constituents and enriches the chemistry of the genus.

3.2. Molecular Docking. The nine isolated compounds have been computationally evaluated using a molecular docking assay for their potential inhibitory effects on four target proteins involved in leishmaniasis and inflammation using Miltefosine® (SD1) and Aspirin® (SD2) as reference drugs (Figure 2). For instance, the protein APRT (PDB ID: 1QCC) is an enzyme causing the pyrophosphorolysis in the sequencing and amplification of nucleic acids in the protein synthesis of *Leishmania donovani* while the enzyme PTR1 (PDB ID: 2XOX) significantly acts in the metacyclogenesis of *Leishmania* [14, 35]. Additionally, human cyclooxygenases 1 and 2 (COX-1 and COX-2) are among the most important mediators of inflammation and have been associated with numerous human diseases including cancer, neurological, and neurodegenerative diseases as well as heart failure.

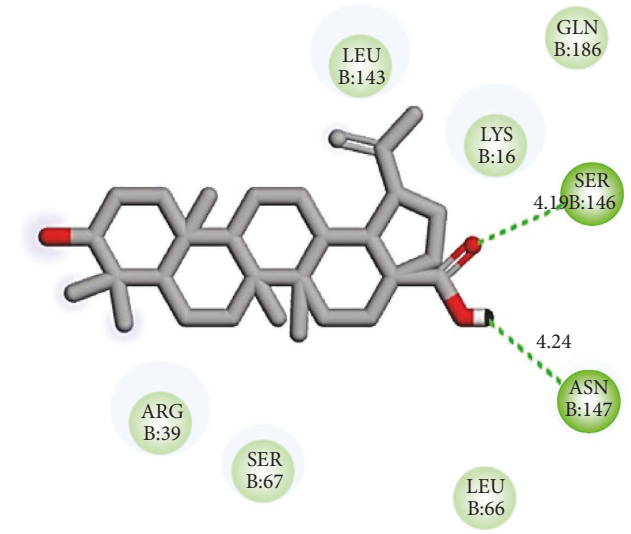

Interactions

van der Waals

Conventional Hydrogen Bond

(a)

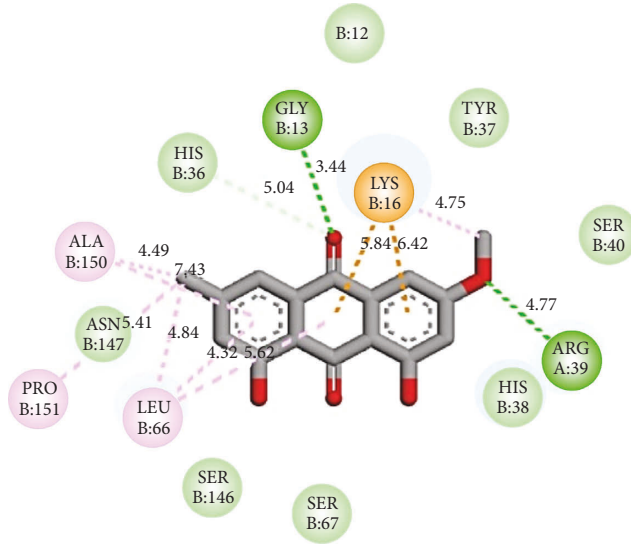

Interactions

van der Waals

Conventional Hydrogen Bond

Carbon Hydrogen Bond

Pi-Cation

Alkyl

Pi-Alkyl

(b)

Figure 5: Continued.

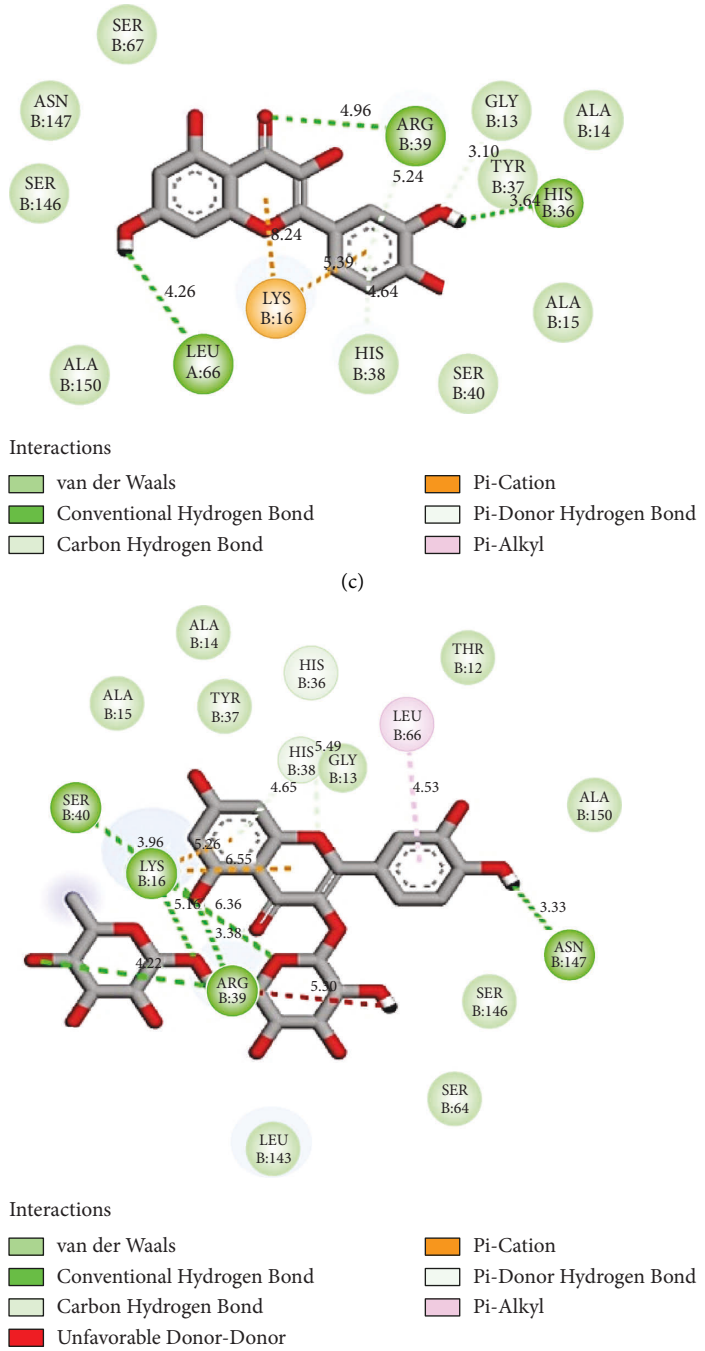

(c)

(d)

Figure 5: Continued.

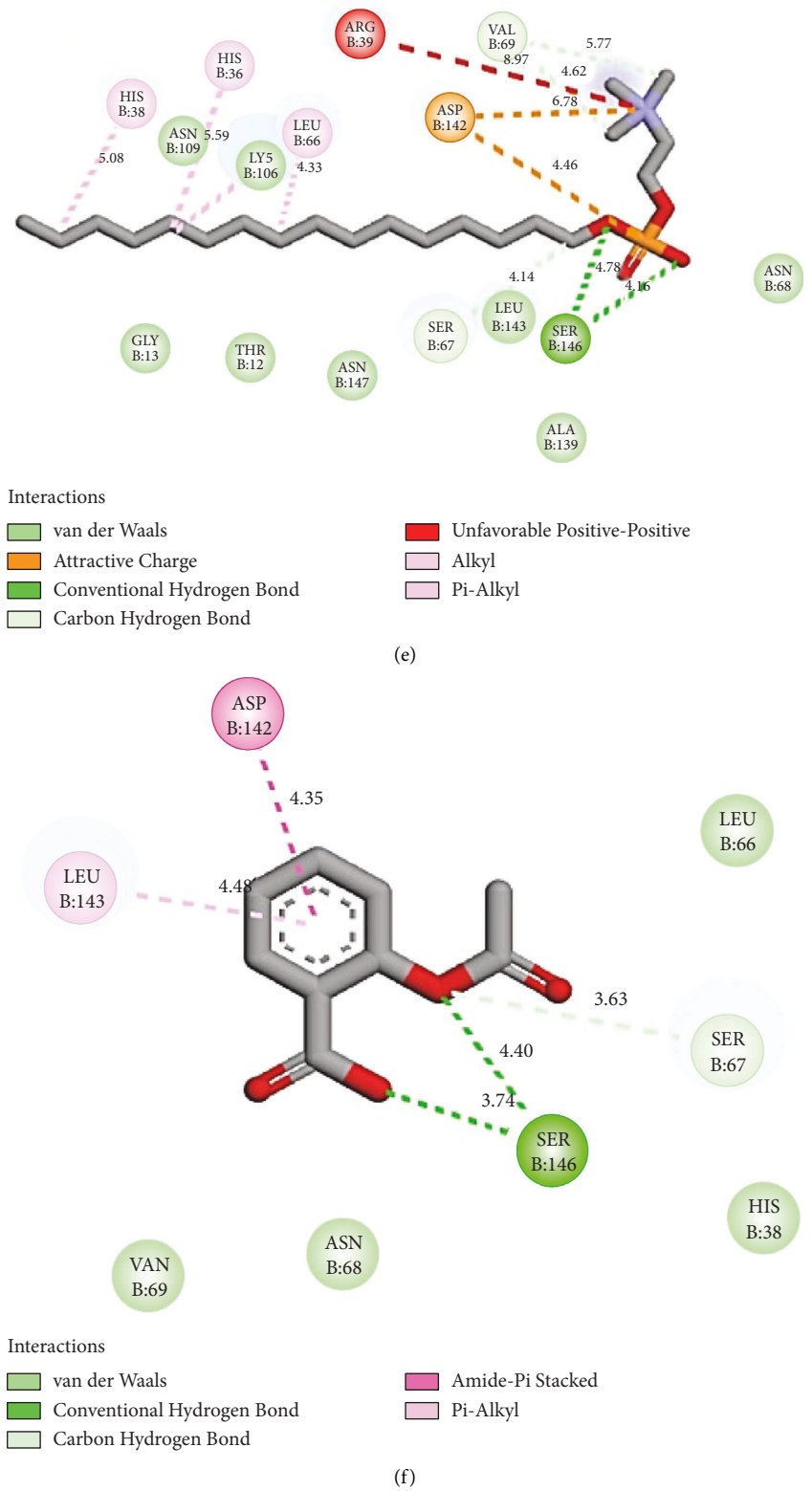

Figure 5: Docking poses of selected compounds at the 2XOX receptor binding site—(a) compound **3**, (b) compound **5**, (c) compound **6**, (d) compound **7**, (e) miltefosine, and (f) aspirin.

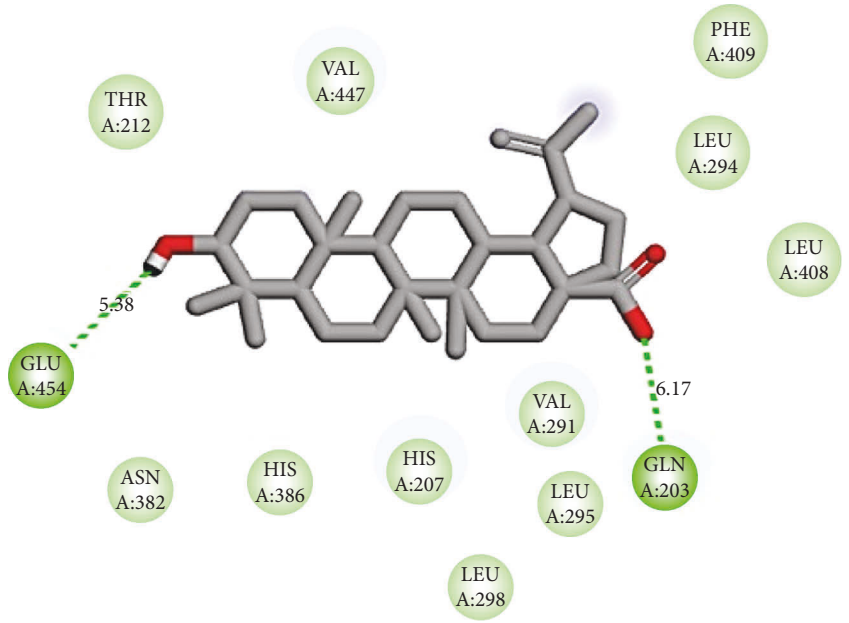

Interactions

van der Waals

Conventional Hydrogen Bond

(a)

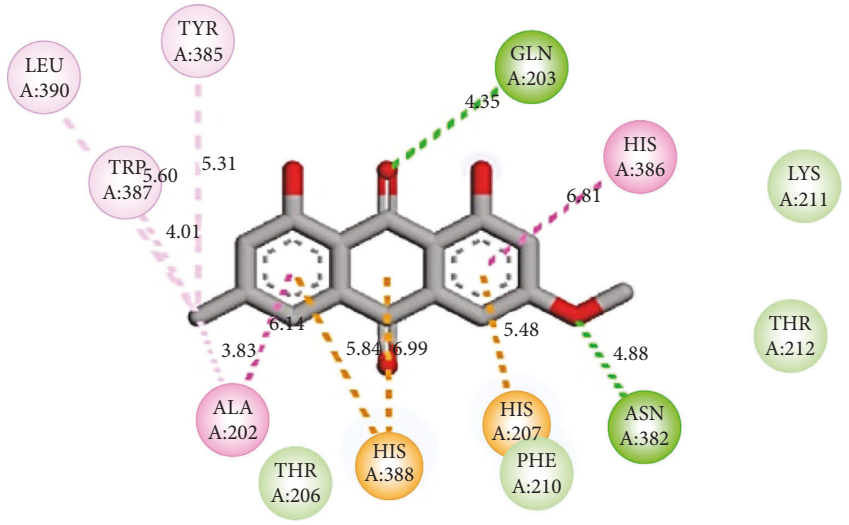

Interactions

van der Waals

Conventional Hydrogen Bond

Pi-Cation

Pi-Pi Stacked

Pi-Pi T-shaped

Amide-Pi Stacked

Alkyl

Pi-Alkyl

(b)

Figure 6: Continued.

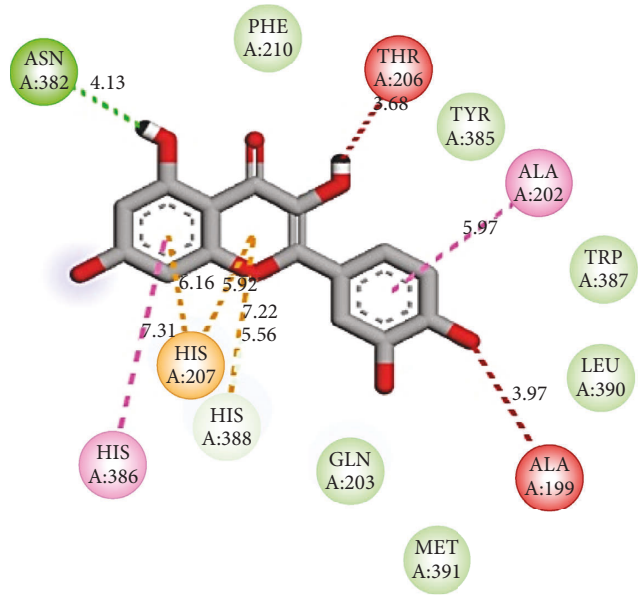

(c)

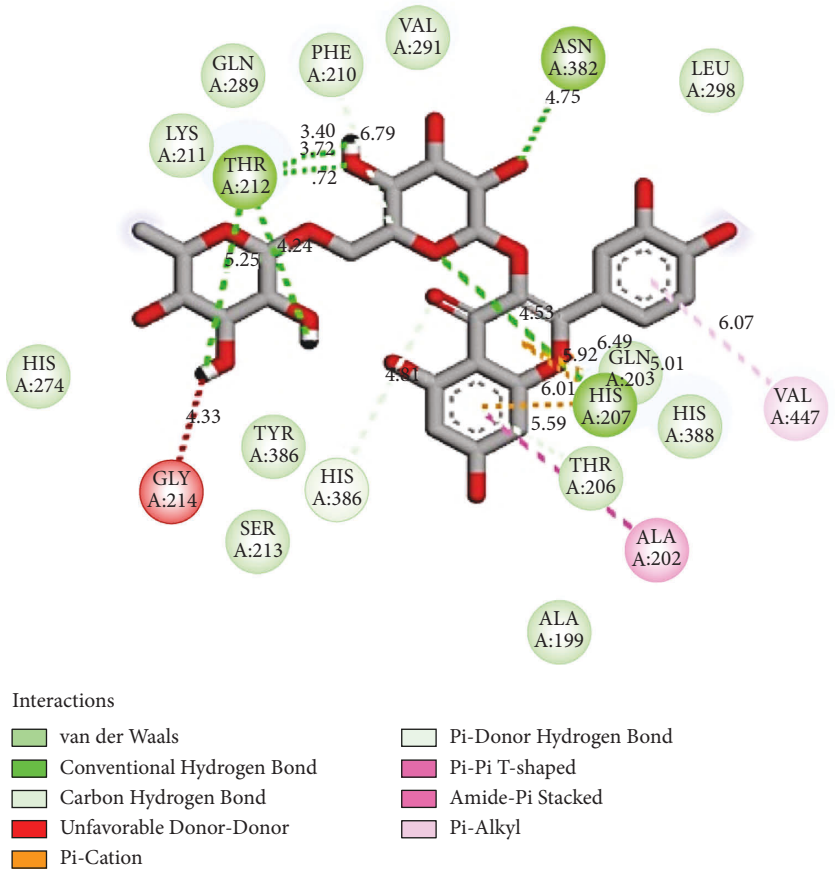

(d)

Figure 6: Continued.

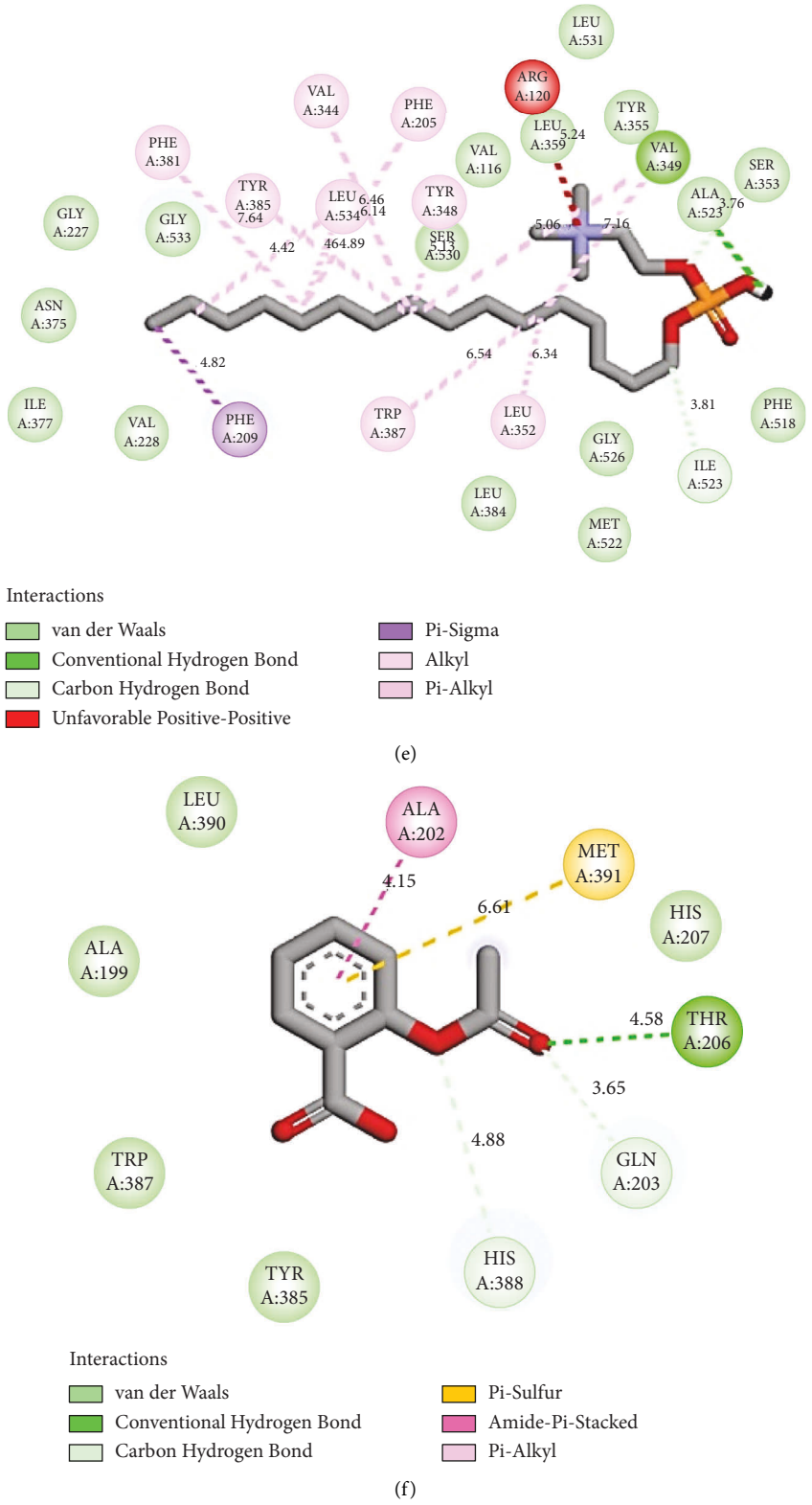

FIGURE 6: Docking poses of selected compounds at the 6Y3C receptor binding site—(a) compound **3**, (b) compound **5**, (c) compound **6**, (d) compound **7**, (e) miltefosine, (f) aspirin.

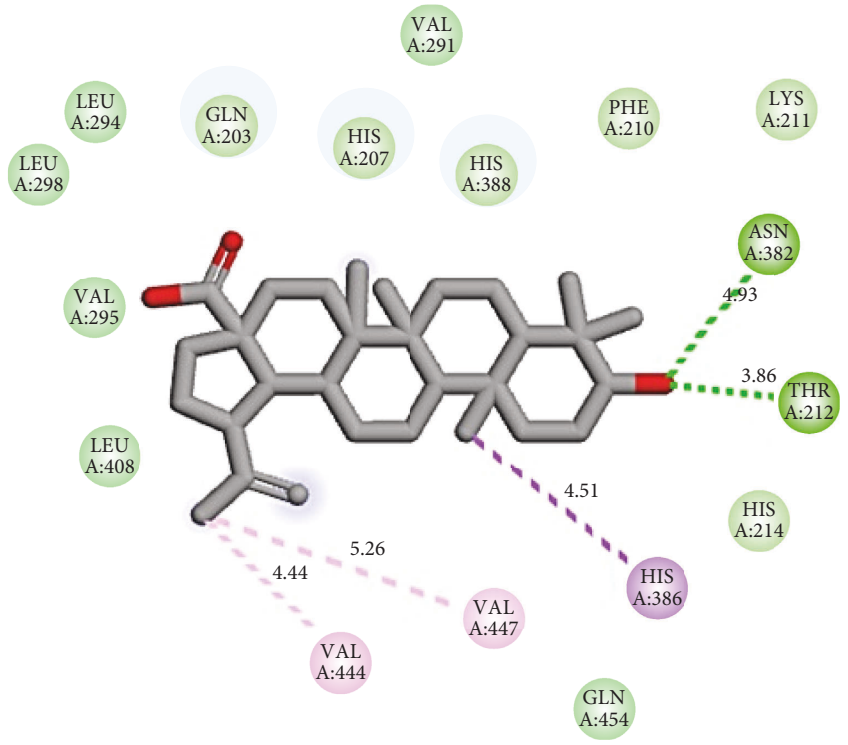

(a)

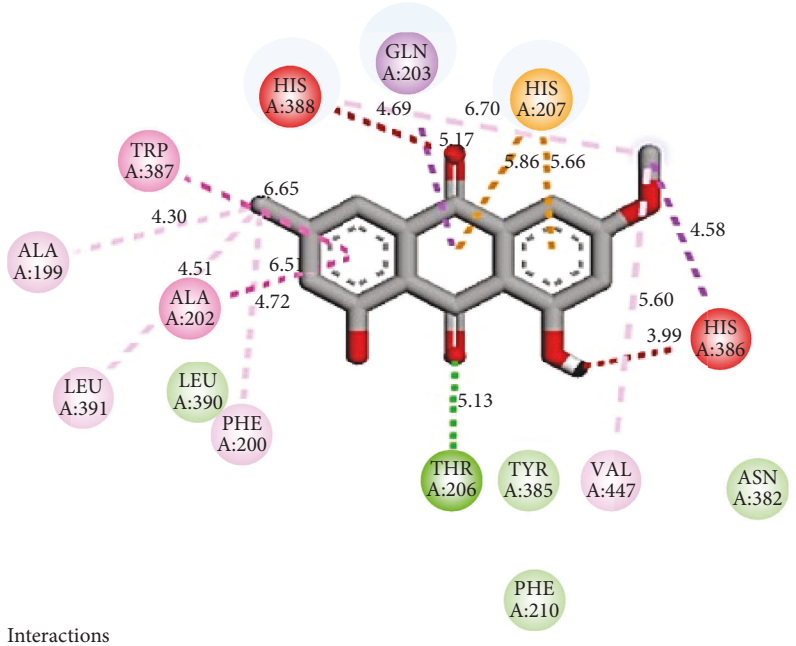

(b)

Figure 7: Continued.

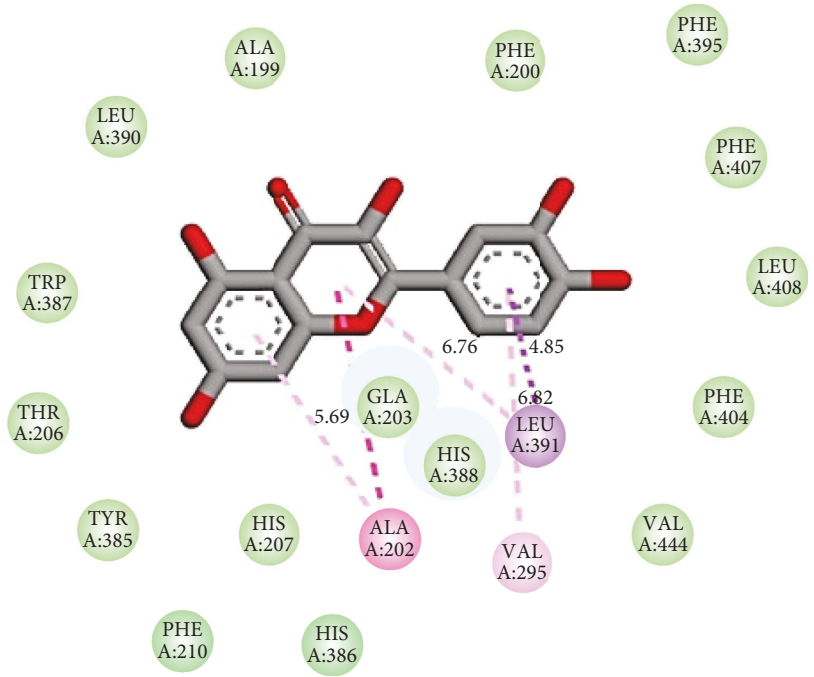

(c)

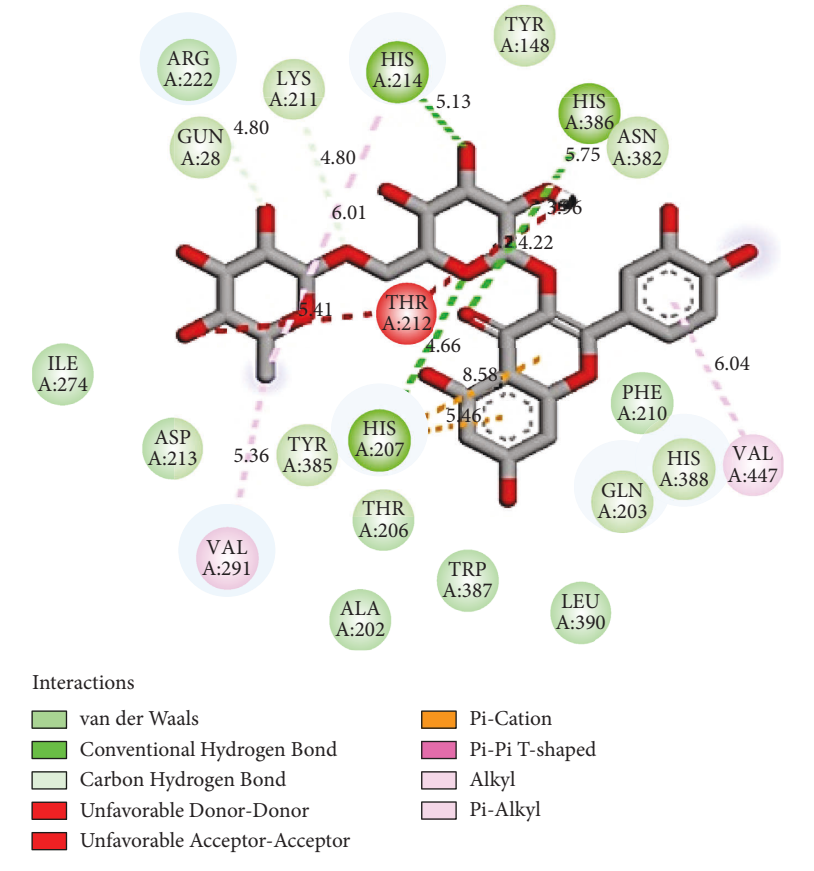

(d)

Figure 7: Continued.

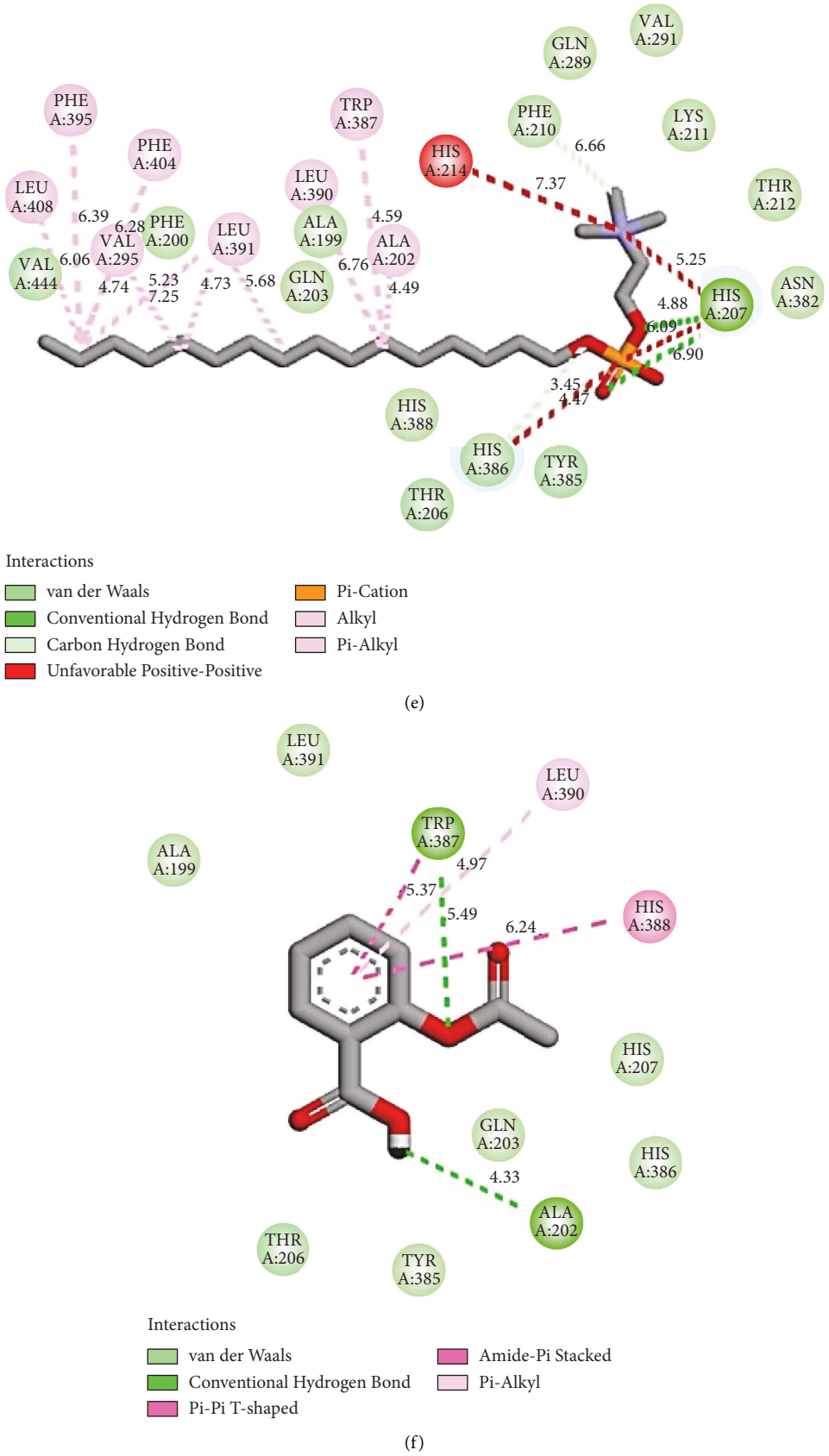

Figure 7: Docking poses of selected compounds at the 1CX2 receptor binding site–(a) compound **3**, (b) compound **5**, (c) compound **6**, (d) compound **7**, (e) miltefosine, and (f) aspirin.

The data presented in Table 2 are the molecular docking scores of the isolated compounds for both antileishmanial and anti-inflammatory receptors. Figure 3 reveals the stacked graphical plot of docking scores. Results revealed that the entire isolated compounds from *Uapaca guineensis* exhibit a better affinity to both antileishmanial receptors' binding sites than Miltefosine® (the standard drug). Likewise, the isolated compounds show a significantly improved affinity to the anti-inflammatory receptors' binding sites compared to Aspirin®.

Figures 4–7 display the binding relationship of four selected compounds (**3**, **5**, **6,** and **7**), and the two standard drugs with the antileishmanial (1QCC.pdb and 2XOX.pdb) and anti-inflammatory (6Y3C.pdb and 1CX2.pdb) receptors while Table 3 reports their contacting residues. Close analysis of the complete docking poses of all 9 compounds (Table 2S in supplementary information file) led to the conclusion that the high receptor-binding affinity of isolated compounds such as **5**, **6**, **7**, and **9** was due to the increase in the hydrogen bonding due to an increase in the number of O-atoms greater than that of the standards. It was also observed that, since nonbonded electrons are far apart from each other, in **5**, **6**, **7**, and **9** hydrogen bonding interactions are seen to be shorter compared to the standard. This result validates the reason for their lower binding energies.

3.3. ADMET Studies. The absorption, distribution, metabolism, excretion, and toxicity (ADMET) studies of the isolated compounds in Table 4 show that the isolated compounds **1**–**8** did not cross the blood brain barrier (BBB violation) which implies that compounds **1**–**8** would not cause addiction when used as lead molecules, whereas aspirin is predicted to violate the BBB over a long term of usage as a drug [36]. The water solubility of all the compounds is seen to fall within the range of −3 to −7 better than that of miltefosine (0.051) and aspirin (–1.650). All isolated compounds are also predicted to have no inhibitors of cytochrome450. Toxicity predictions infer that all the selected compounds are not blockers of the human either–a–go–a–go heart function and they are predicted to be nontoxic if applied as drugs. The toxicity ratings for all isolated compounds can therefore be improved during the further drug design optimization process, as it was done with miltefosine and aspirin.

4. Conclusion

During the chemical investigations of the root bark of *Uapaca guineensis*, nine compounds have been isolated and characterized as lupeol (**1**), betulin (**2**), betulinic acid (**3**), β-amyryl acetate (**4**), physcion (**5**), quercetin (**6**), rutin (**7**), β-sitosterol (**8**), and β-sitosterol-3-*O*-β-D-glucopyranoside (**9**), respectively. Although all the compounds are reported for the first time from the species *U. guineensis*, the lupane-type triterpenoids **1**–**3** have been obtained from *U. paludosa*, while compounds **4** and **9** have been reported from *U. togoensis,* and some structurally close flavonoids to **6** and **7** have been obtained from *U. heudelotti*. This study strengthens the taxonomy of the plant based on its chemical markers and enriches the chemistry of the plant genus *Uapaca*. Furthermore, all the isolated compounds have been computationally evaluated for their ability to inhibit the receptors 1QCC and 2XOX (for the antileishmanial studies) and 6Y3C and 1CX2 (for the anti-inflammatory studies). The results showed that all the compounds have a better affinity to both receptor's binding sites than the standard drugs miltefosine and aspirin and might not cause addiction when used as lead molecules, whereas aspirin is predicted to violate the BBB over a long term of usage as a drug. Although *in vitro* and *in vivo* studies are important to support the *in silico* results, the current results are important in supporting the use of the plant in traditional medicine for the treatment of skin diseases, leishmaniasis, and inflammatory diseases as well as giving further insights into the development of new potent drugs.

Data Availability

The molecular docking data of all the isolated compounds and their spectroscopic (^{1}H and ^{13}C NMR) data used to support the findings of this study are included within the supplementary information file.

Conflicts of Interest

The authors declare that they have no conflicts of interest.

Supplementary Materials

Section A: Molecular docking data. Figure 1S: Graphical relationship between isolated compounds and binding affinity (or binding energy). Table 1S: Simile notations of the isolated compounds used for ADMET studies. Table 2S: 2D-plot binding interactions between isolated compounds and selected receptors. Section B: NMR spectra of isolated compounds. Figure 2S: ^{1}H NMR spectrum of lupeol (1) in CDCl3. Figure 3S: ^{13}C NMR spectrum of lupeol (1) in CDCl3. Figure 4S: ^{1}H NMR spectrum of betulin (2) in CDCl3. Figure 5S: ^{13}C NMR spectrum of betulin (2) in CDCl3. Figure 6S: 1H NMR spectrum of betulinic acid (3) in CD3OD + CDCl3. Figure 7S: ^{13}C NMR spectrum of betulinic acid (3) in CD3OD + CDCl3. Figure 8S: ^{1}H NMR spectrum of β-amyryl acetate (4) in CDCl3. Figure 9S: Enlarged ^{1}H NMR spectrum of β-amyryl acetate (4) in CDCl3. Figure 10S: ^{13}C NMR spectrum of β-amyryl acetate (4) in CDCl3. Figure 11S: ^{1}H NMR spectrum of physcion (5) in CDCl3. Figure 12S: ^{13}C NMR spectrum of physcion (5) in CDCl3. Figure 13S: ^{1}H NMR spectrum of quercetin (6) in CD3OD + CDCl3. Figure 14S: ^{13}C NMR spectrum of quercetin (6) in CD3OD + CDCl3. Figure 15S: ^{1}H NMR spectrum of rutin (7) in CD3OD. Figure 16S: 13C NMR spectrum of rutin (7) in CD3OD. Figure 17S: ^{13}C DEPT 135 NMR spectrum of rutin (7) in CD3OD. Figure 18S: ^{1}H NMR spectrum of β-sitosterol (8) in CD3OD. Figure 19S: EI-MS

spectrum of β-sitosterol (8). Figure 20S: ^{1}H NMR spectrum of daucosterol (9) in CD3OD + CDCl3. Figure 21S: ^{13}C NMR spectrum of daucosterol (9) in CD3OD + CDCl3. Figure 22S: ^{13}C DEPT 135 NMR spectrum of daucosterol (9) in CD3OD + CDCl3. (*Supplementary Materials*)

References

[1] S. Burza, S. L. Croft, and M. Boelaert, "Leishmaniasis," *Lancet*, vol. 392, no. 10151, pp. 951–970, 2018.

[2] F. Chappuis, S. Sundar, A. Hailu et al., "Visceral leishmaniasis: what are the needs for diagnosis, treatment and control?" *Nature Reviews Microbiology*, vol. 5, no. S11, pp. S7–S16, 2007.

[3] B. Zulfiqar, T. B. Shelper, and V. M. Avery, "Leishmaniasis drug discovery: recent progress and challenges in assay development," *Drug Discovery Today*, vol. 22, no. 10, pp. 1516–1531, 2017.

[4] A. Das, J. J. Jawed, M. C. Das et al., "Antileishmanial and immunomodulatory activities of lupeol, a triterpene compound isolated from *Sterculia villosa*"," *International Journal of Antimicrobial Agents*, vol. 50, no. 4, pp. 512–522, 2017.

[5] D. C. Rubin, A. Shaker, and M. S. Levin, "Chronic intestinal inflammation: inflammatory bowel disease and colitis-associated colon cancer," *Frontiers in Immunology*, vol. 3, no. 107, p. 107, 2012.

[6] S. Harirforoosh, W. Asghar, and F. Jamali, "Adverse effects of nonsteroidal antiinflammatory drugs: an update of gastrointestinal, cardiovascular and renal complications," *Journal of Pharmacy & Pharmaceutical Sciences*, vol. 16, no. 5, p. 821, 2014.

[7] G. M. Happi, P. K. Nangmo, L. C. Dzouemo, S. F. Kache, A. D. K. Kouam, and J. D. Wansi, "Contribution of Meliaceous plants in furnishing lead compounds for antiplasmodial and insecticidal drug development," *Journal of Ethnopharmacology*, vol. 285, Article ID 114906, 2022.

[8] G. M. Happi, V. K. Ntabo, A. T. Tcho, and J. D. Wansi, "Naturally occurring dimeric triterpenoids: Occurrence, chemistry and bioactivities," *Phytochemistry*, vol. 200, Article ID 113242, 2022.

[9] V. Kimpouni, "Contribution aux etudes ethnobotaniques et floristiques de la foret de Lossi (R.P. Congo): les plantes de cueillette a usage alimentaire," *Systematics and Geography of Plants*, vol. 71, no. 2, p. 679, 2001.

[10] A. Bouquet and M. Debray, "Plantes médicinales de la Côte d'Ivoire," *Travaux et Documents de l' O.R.S.T.O.M., Paris*, vol. 32232 pages, 1974.

[11] N. Mills, *ChemDraw Ultra 10.0 CambridgeSoft, 100 CambridgePark Drive*, ACS Publications, Cambridge, MA, USA, 2006.

[12] M. D. Hanwell, D. E. Curtis, D. C. Lonie, T. Vandermeersch, E. Zurek, and G. R. Hutchison, "Avogadro: an advanced semantic chemical editor, visualization, and analysis platform," *Journal of Cheminformatics*, vol. 4, p. 17, 2012.

[13] C. L. Phillips, B. Ullman, R. G. Brennan, and C. P. Hill, "Crystal structures of adenine phosphoribosyltransferase from *Leishmania donovani*"," *The EMBO Journal*, vol. 18, no. 13, pp. 3533–3545, 1999.

[14] K. L. Barrack, L. B. Tulloch, L. A. Burke, P. K. Fyfe, and W. N. Hunter, "Structure of recombinant *Leishmania donovani* pteridine reductase reveals a disordered active site," *Acta Crystallographica, Section F: Structural Biology and Crystallization Communications*, vol. 67, no. 1, pp. 33–37, 2011.

[15] M. Miciaccia, B. D. Belviso, M. Iaselli et al., "Three-dimensional structure of human cyclooxygenase (hCOX)-1," *Scientific Reports*, vol. 11, no. 1, 2021.

[16] S. S. u. Hassan, W. D. Zhang, H.-Z. Jin, S. H. Basha, and S. V. S. S. Priya, "*In-silico* anti-inflammatory potential of guaiane dimers from *Xylopia vielana* targeting COX-2," *Journal of Biomolecular Structure and Dynamics*, vol. 40, no. 1, pp. 484–498, 2022.

[17] D. Biovia, *BIOVIA Pipeline Pilot*, Dassault Systèmes, San Diego, CA, USA, 2021.

[18] S. Dallakyan and A. J. Olson, "Small-molecule Library Screening by Docking with PyRx," *Chemical Biology*, vol. 1263, pp. 243–250, 2015.

[19] O. Trott and A. J. Olson, "Software news and update autodockvina: improving the speed and accuracy of docking with a new scoring function, efficient optimization, and multithreading," *Journal of Computational Chemistry*, vol. 31, pp. 455–461, 2010.

[20] H. Wickham, W. Chang, and M. H. Wickham, "Package 'ggplot2'," *Create Elegant Data Visualisations Using the Grammar of Graphics"*, vol. 2, pp. 1–189, 2016.

[21] G. Xiong, Z. Wu, J. Yi et al., "ADMETlab 2.0: an integrated online platform for accurate and comprehensive predictions of ADMET properties," *Nucleic Acids Research*, vol. 49, no. W1, pp. W5–W14, 2021.

[22] M. L. D. Miranda, F. R. Garcez, and W. S. Garcez, "Triterpenes and other constituents from fruits of *Enterolobium contortisiliquum* (vell.) morong (fabaceae)," *Revista Virtual de Quimica*, vol. 7, no. 6, pp. 2597–2605, 2015.

[23] L. V. L. Bongmo, A. B. Nouga, G. M. Happi et al., "Phytochemical compounds of *Guibourtia ehie* and their antioxidant, urease and α-glucosidase inhibitory activities," *Natural Resources for Human Health*, vol. 2, no. 3, pp. 306–312, 2022.

[24] A. A. Ahmadu, C. Delehouze, A. Haruna et al., "Betulin, a newly characterized compound in *Acacia auriculiformis* bark, is a multi-target protein kinase inhibitor," *Molecules*, vol. 26, no. 15, 2021.

[25] G. M. Happi, A. S. W. Mbobda, M. Frese et al., "A new phenylpropanoid glycoside from *Psorospermum tenuifolium* Kotschy (Hypericaceae)," *Trends of Phytochemical Research*, vol. 5, 2021.

[26] A. Wahab Obeng, Y. D. Boakye, T. A. Agana, G. I. Djameh, D. Boamah, and F. Adu, "Anti-trypanosomal and anthelminthic properties of ethanol and aqueous extracts of *Tetrapleura tetraptera* Taub," *Veterinary Parasitology*, vol. 294, Article ID 109449, 2021.

[27] G. M. Happi, G. P. Mouthe Kemayou, H.-G. Stammler et al., "Three phragmalin-type limonoids orthoesters and the structure of odoratone isolated from the bark of *Entandrophragma candollei* (Meliaceae)," *Phytochemistry*, vol. 181, Article ID 112537, 2021.

[28] J.-W. Dong, L. Cai, Y.-S. Fang, W.-H. Duan, Z.-J. Li, and Z.-T. Ding, "Simultaneous, simple and rapid determination of five bioactive free anthraquinones in radix et rhizoma rhei by quantitative ^{1}H NMR," *Journal of the Brazilian Chemical Society*, vol. 27, 2016.

[29] Y. Zhang, D. Wang, L. Yang, D. Zhou, and J. Zhang, "Purification and characterization of flavonoids from the leaves of *Zanthoxylum bungeanum* and correlation between their structure and antioxidant activity," *PLoS One*, vol. 9, no. 8, Article ID e105725, 2014.

[30] G. M. Happi, S. C. N. Wouamba, M. Ismail et al., "Ergostane-type steroids from the Cameroonian 'white tiama'

Entandrophragma angolense," *Steroids*, vol. 156, Article ID 108584, 2020.

[31] B. Nyasse, J.-J. Nono, Y. Nganso, I. Ngantchou, and B. Schneider, "*Uapaca* genus (Euphorbiaceae), a good source of betulinic acid," *Fitoterapia*, vol. 80, no. 1, pp. 32–34, 2009.

[32] J. T. Banzouzi, P. N. Soh, S. Ramos et al., "Samvisterin, a new natural antiplasmodial betulin derivative from *Uapaca paludosa* (Euphorbiaceae)," *Journal of Ethnopharmacology*, vol. 173, pp. 100–104, 2015.

[33] V. Kuete, L. P. Sandjo, J. A. Seukep et al., "Cytotoxic Compounds from the Fruits of *Uapaca togoensis* towards multifactorial drug-resistant cancer cells," *Planta Medica*, vol. 81, no. 01, pp. 32–38, 2014.

[34] J. I. Achika, R. G. Ayo, A. O. Oyewale, and J. D. Habila, "Flavonoids with antibacterial and antioxidant potentials from the stem bark of *Uapaca heudelotti*"," *Heliyon*, vol. 6, no. 2, Article ID e03381, 2020.

[35] Z. Zaheer, F. A. K. Khan, J. N. Sangshetti, and R. H. Patil, "Expeditious synthesis, antileishmanial and antioxidant activities of novel 3-substituted-4-hydroxycoumarin derivatives," *Chinese Chemical Letters*, vol. 27, no. 2, pp. 287–294, 2016.

[36] A. Daina, O. Michielin, and V. Zoete, "SwissADME: a free web tool to evaluate pharmacokinetics, drug-likeness and medicinal chemistry friendliness of small molecules," *Scientific Reports*, vol. 7, no. 1, Article ID 42717, 2017.